The impact of jamming on boundaries of collectively moving weak-interacting cells

**Kenechukwu David Nnetu[1], Melanie Knorr, Josef Käs
and Mareike Zink**

Institut für Experimentelle Physik I, Universität Leipzig, D-04103 Leipzig,
Germany
E-mail: nnetu@physik.uni-leipzig.de

Abstract. Collective cell migration is an important feature of wound healing, as well as embryonic and tumor development. The origin of collective cell migration is mainly intercellular interactions through effects such as a line tension preventing cells from detaching from the boundary. In contrast, in this study, we show for the first time that the formation of a constant cell front of a monolayer can also be maintained by the dynamics of the underlying migrating single cells. Ballistic motion enables the maintenance of the integrity of the sheet, while a slowed down dynamics and glass-like behavior cause jamming of cells at the front when two monolayers—even of the same cell type—meet. By employing a velocity autocorrelation function to investigate the cell dynamics in detail, we found a compressed exponential decay as described by the Kohlrausch–William–Watts function of the form $C(\delta x)_t \sim \exp\left(-(x/x_0(t))^{\beta(t)}\right)$, with $1.5 \leqslant \beta(t) \leqslant 1.8$. This clearly shows that although migrating cells are an active, non-equilibrium system, the cell monolayer behaves in a glass-like way, which requires jamming as a part of intercellular interactions. Since it is the dynamics which determine the integrity of the cell sheet and its front for weakly interacting cells, it becomes evident why changes of the migratory behavior during epithelial to mesenchymal transition can result in the escape of single cells and metastasis.

S Online supplementary data available from stacks.iop.org/NJP/14/115012/mmedia

---

[1] Author to whom any correspondence should be addressed.

IOP Institute of Physics **Φ** DEUTSCHE PHYSIKALISCHE GESELLSCHAFT

Contents

1. Introduction

Collective cell migration is an important characteristic of morphogenesis, wound healing and the growth of a tumor front [1, 2]. However, the origins of cooperative motion such as cell signaling processes and physical forces are still under debate and not fully understood [3–7]. The molecular and cellular mechanisms underlying collective cell migration require cell–cell cohesion, collective polarization and the coordination of cytoskeletal activities resulting in the generation of shear and traction forces within the monolayer [8–10]. This shear force can result in plithotaxis [8]. Classically, the integrity of the monolayer during migration is retained by cell–cell cohesion. It is therefore conceivable that epithelial to mesenchymal transition can only occur when single cells are capable of overcoming the boundary of the migrating monolayer. This concept was verified by studies in which single cells were able to escape an initially intact monolayer upon the addition of trypsin to the medium [11]. Chemicals such as trypsin down-regulate intercellular interactions and change the physical properties of the monolayer, especially the line tension, preventing cells from escaping the sheet. In contrast, fibroblast cells were shown not to migrate collectively; single cells detach from the monolayer and no smooth cell front is sustained [11, 12].

Although intercellular interactions are important in maintaining the integrity of a migrating cell monolayer, the dynamic interplay between escaping single cells and the monolayer is also sufficient to maintain a constant cell front during collective cell migration. It was recently shown with a wound-healing-like assay that cells collectively migrating into free space move ballistically, while escaping single cells migrate randomly on long times [12]. This ballistic motion of the monolayer allows it to catch up with escaping single cells and a constant boundary and line tension during migration is observed.

The maintenance of a constant cell boundary is necessary for early stages of cancer when tumor cells remain within the growing host tumor and separate from the normal tissue surrounding it. In contrast to the described dynamically induced stabilization of boundaries [12], the differential adhesion hypothesis describes tissue demixing and boundary stabilization in three dimensions from a static force point of view [13]. Here cells and tissues exhibit a liquid-like behavior and are capable of demixing based on their mutual affinity [14, 15], while cells

of the same type prefer to cohere with each other instead of adhering to cells of another type. The adhesion difference between different cell types initiates cell sorting, which results in the separation of cells. The cell type with the lower surface tension envelopes the one with a higher surface tension. To this end, a constant cell boundary between both cell types is formed. There have been extensive experimental and theoretical studies [16] that demonstrated the importance of cell sorting through intercellular interactions and contractility in embryogenesis and cancer dissemination [17]. This three-dimensional (3D) cell sorting concept was extended to two-dimensional (2D) cell monolayers [18–20]. In 2D, the adhesive difference between the cells and the substrate on which they migrate determines whether the cells form a monolayer or round up to form a 3D tissue. However, to what extent physical properties account for cell separation and their impact on collective cell migration remains an open question.

To study the impact of adhesive differences on the stabilization of boundaries, we used the non-malignant epithelial cell line MCF-10A and the malignantly transformed epithelial cell line MCF-7. MCF-7 epithelial cells are expected to have weaker intercellular interactions in comparison with MCF-10A cells since the metastatic potential of the former should reduce their intercellular interactions [21, 22]. Contrary to epithelial cells, fibroblasts *in vivo* do not form monolayers and have been shown *in vitro* to migrate diffusively upon the provision of free space. Therefore, we additionally employ NIH-3t3 fibroblasts to assess their migratory behavior. It is expected that the intercellular interactions between these cells should be very weak and the cells should not generally migrate collectively.

Glass-like effects were recently shown in collectively migrating cells [23]. However, these effects were employed for the center of a cell monolayer. This naturally raises the question: since a monolayer has a packing fraction of one, are jamming and glass-like effects occurring in a wound-healing-like assay? In this study, in contrast to a fibroblast monolayer in which cells do not migrate collectively, we find that glass-like effects occur in a migrating epithelial MCF-10A cell monolayer. Here the boundary of the monolayer was stable during migration due to ballistic motion of the underlying cells, while slowed down dynamics and jamming led to the formation of stable borders between two monolayers—even of the same cell type. We further characterized the collective dynamics by correlation functions, which could be fitted by compressed exponential functions of the Kohlrausch–William–Watts type. Thus, in contrast to the predictions of the differential adhesion hypothesis, jamming seems to stabilize the boundary even of weakly interacting cells within the monolayer when two counter propagating monolayers meet.

2. Materials and methods

2.1. Cell culture

MCF-10A epithelial cell lines (ATCC) were cultured in Dulbecco's modified Eagle's medium and Ham's F12 medium (PAA, B11-035), supplemented with 20 ng ml^{-1} human epidermal growth factor (Gibco, PHG0311), 100 ng ml^{-1} Cholera toxin (Sigma-Aldrich), 0.01 mg ml^{-1} insulin (Sigma-Aldrich), 500 ng ml^{-1} hydrocortisone and 5% horse serum (ATCC/LGC Promochem, 30-2040).

The MCF-7 cell line was bought from ATCC; it was cultured with Minimal Essential Medium Eagle's with L-glutamine and Earle's salt and was supplemented with sodium pyruvate,

IOP Institute of Physics Φ DEUTSCHE PHYSIKALISCHE GESELLSCHAFT

bovine insulin, non-essential amino acids, foetal bovine serum and penicillin/streptomycin. Epithelial cells generally migrate together since they strongly express cadherin proteins.

The NIH-3t3 fibroblast cell line was cultured in Dulbecco's Modified Eagle's Medium supplemented with 10% bovine calf serum. All the cell lines were cultured at $37\,^\circ$C, with 5% CO_2 in an incubator, while media were changed every second day.

2.2. Phase contrast time lapse microscopy

For phase contrast microscopy migratory measurements, cells were washed with phosphate buffer saline, trypsinized, centrifugated and re-suspended in the culture medium. Cells were counted using a hemocytometer and seeded in an ibidi (München, Germany; product number: 80241) culture insert attached to a Nunc culture dish. The cells were allowed to attach, divide and form a monolayer by incubation at $37\,^\circ$C with 5% CO_2 after which the insert was removed and the dish placed on an inverted microscope (DMIRB, Leica) containing a custom made heater kept at $37\,^\circ$C and supplied with 5% CO_2 in air. A frame was taken every 5 min (using a Dalsa DS-21-02M30 CCD camera (Dalsa Corporation), $10\times$ objective with NA 0.3 and a $0.5\times$ C-mount) for the epithelial cells and every 2 min for the fibroblast cells. Each measurement lasted 48 h.

## 2.3. Mapping of displacement fields and spatial velocity distribution

To obtain the spatio-temporal velocity distribution, a mesh grid of distance $10\,\mu$m was defined on the cell monolayer images. At each grid point, a template pixel area ($\mathbf{M}$) of size $20 \times 20\,\mu$m^2 was cropped. $\mathbf{M}$ was overlaid and scanned through a larger search area ($\mathbf{S}$) at the same grid point in the succeeding image. The size of $\mathbf{S}$ was $5\,\mu$m larger than $\mathbf{M}$. A 2D-cross-correlation algorithm determined the pixel area in $\mathbf{S}$ that is most common with $\mathbf{M}$. The cross-correlation was defined as

$$C_{mn} = \frac{\sum_m \sum_n (\mathbf{M}_{mn} - \bar{\mathbf{M}})(\mathbf{S}_{mn} - \bar{\mathbf{S}})}{\sqrt{\sum_m \sum_n (\mathbf{M}_{mn} - \mathbf{M})^2 (\mathbf{S}_{mn} - \bar{\mathbf{S}})^2}}, \tag{1}$$

where m and n are the position indices of each image point and $\bar{\mathbf{M}}$ and $\bar{\mathbf{S}}$ denote the average values of $\mathbf{M}$ and $\mathbf{S}$. The position of maximum cross-correlation value in $\mathbf{S}$ defines the displacement vector of each grid point. This determines the movement of a cell within the monolayer from one image to the next and results in a discrete displacement vector field defined as

$$\Delta r_{mn}(t) = \sum_m \sum_n \left(r_{mn}(t + \delta t) - r_{mn}(t) \right), \tag{2}$$

where $r(x(t), y(t)) = (x(t), y(t))$. A 3D convolution kernel was used on the discrete displacement field interpolating to obtain the final flow field. This convolution kernel is a normalized Gaussian ranging ± 2 frames in time with a variance of one frame. The spatial variance of the kernel was $20\,\mu$m. Furthermore, the convolution is only done for discrete displacements with a cross-correlation value above 0.7. The software is described in [24, 25] in detail.
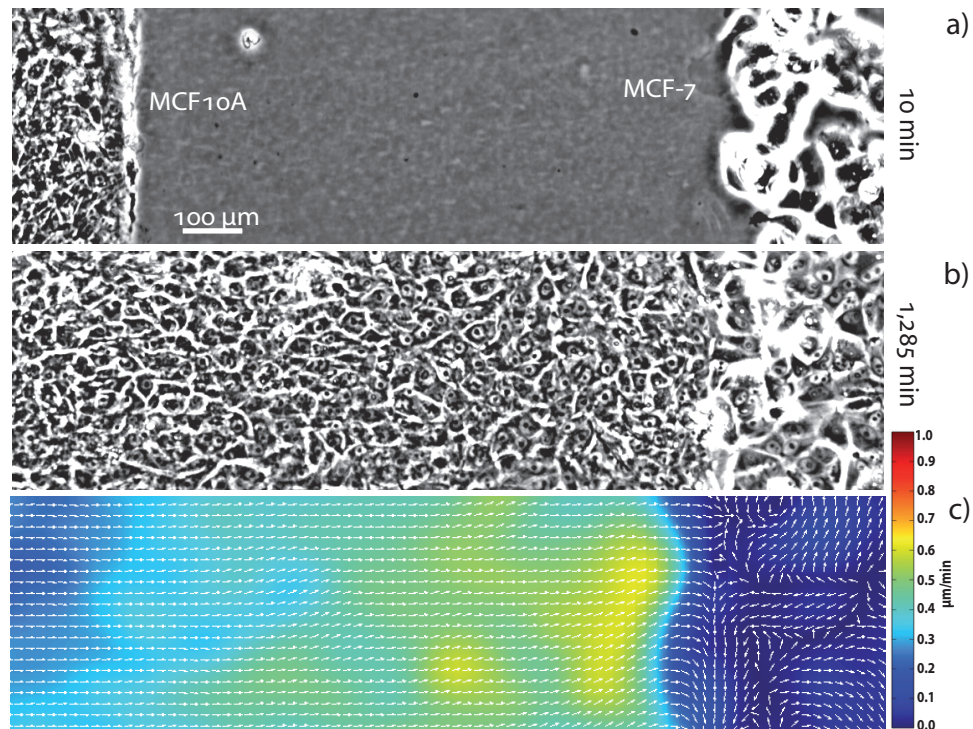
Figure 1. Phase contrast image of an MCF-10A and MCF-7 monolayer at various times. Panels (a) and (b) are phase contrast images of the MCF-10A (left) and MCF-7 (right) monolayers at times 10 and 1285 min, respectively. While the MCF-10A monolayer was motile over time, the MCF-7 was stationary throughout the measurement. Panel (c) is the spatial velocity distribution of the monolayers. The velocity of the MCF-10A monolayer was spatially heterogeneous from the front to the back of the monolayer. The white arrows indicate the displacement field of the monolayer for time 1285 min.

3. Results

3.1. Boundary stabilization

To gain insight into the collective properties of migrating MCF-10A and MCF-7 epithelial cells, we performed a wound-healing-like assay in which both cell types were employed as monolayers, migrating in opposite directions towards each other. We first observed that MCF-10A and MCF-7 cell layers formed stable boundaries (figures 1(a) and (b)), and the MCF-10A monolayer migrated faster than the MCF-7 cell. Indeed, the MCF-7 monolayer was stationary and no dynamics of the sheet itself became visible. When the boundary of the MCF-10A monolayer met the MCF-7 borderline, no mixing between the monolayers was evident (figure 1(b), see supplementary data, movie 1 (available from stacks.iop.org/NJP/14/115012/mmedia)). The velocity (color coded in figure 1(c)) of the MCF-10A monolayer was spatially and temporally heterogeneous, while the displacement fields (white arrows in figure 1(c)) of the monolayer were uni-directional and indicated directed persistent (ballistic) motion during migration.
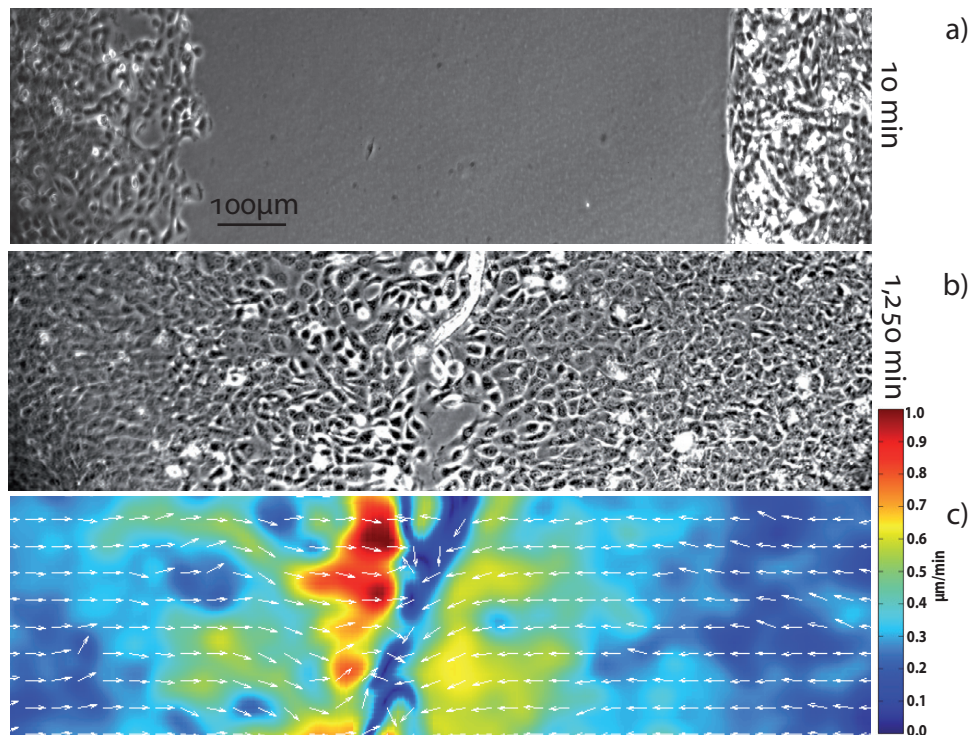
Figure 2. Phase contrast images of two oppositely migrating MCF-10A monolayers. Panels (a) and (b) are the phase contrast images of the MCF-10A monolayer at times 10 and 1250 min, respectively. It should be noted that the density on the left-hand side is lower (5×10^3 cells cm^{-2}) than that of the right-hand side (2×10^5 cells cm^{-2}). At the lower cell density, single cells could escape the monolayer. Panel (c) is the spatial velocity distribution of the monolayer after 1250 min. The velocities are both spatially heterogeneous and the displacement fields (white arrows) are uni-directional.

To verify if the lack of mixing of both monolayers emanates from the jammed nature of the monolayer and the strong intercellular interactions between the cells and not from the differential adhesiveness of the two cell types as postulated by the differential adhesion hypothesis, we employed the same wound-healing-like assay, but with MCF-10A cells on both sides. Thus, two MCF-10A monolayers migrated towards each other, while imaging the interaction of the sheet fronts and the dynamics of single cells after the incidence of the two monolayers. As shown in figures 2(a) and (b), no mixing of cells originating from oppositely migrating MCF-10A monolayers was present and the cells remained within their initial cell sheet (supplementary movie 2, available from stacks.iop.org/NJP/14/115012/mmedia). The cell density within the monolayer on the left-hand side (figure 2(a)) was lower (5×10^3 cells cm^{-2}) compared to the density on the right side (2×10^5 cells cm^{-2}). This variation in density originated in different single cell dynamics: while in the lower cell density sheet, single cells could escape during migration, such single cell motion out of the sheet was not evident for the high-density layer. The spatial velocity distribution of both monolayers was identical to the distribution of MCF-10A cells as shown in figure 1(c); the displacement fields were uni-directional, thus indicating ballistic motions. Due to this directionality, both monolayers retained
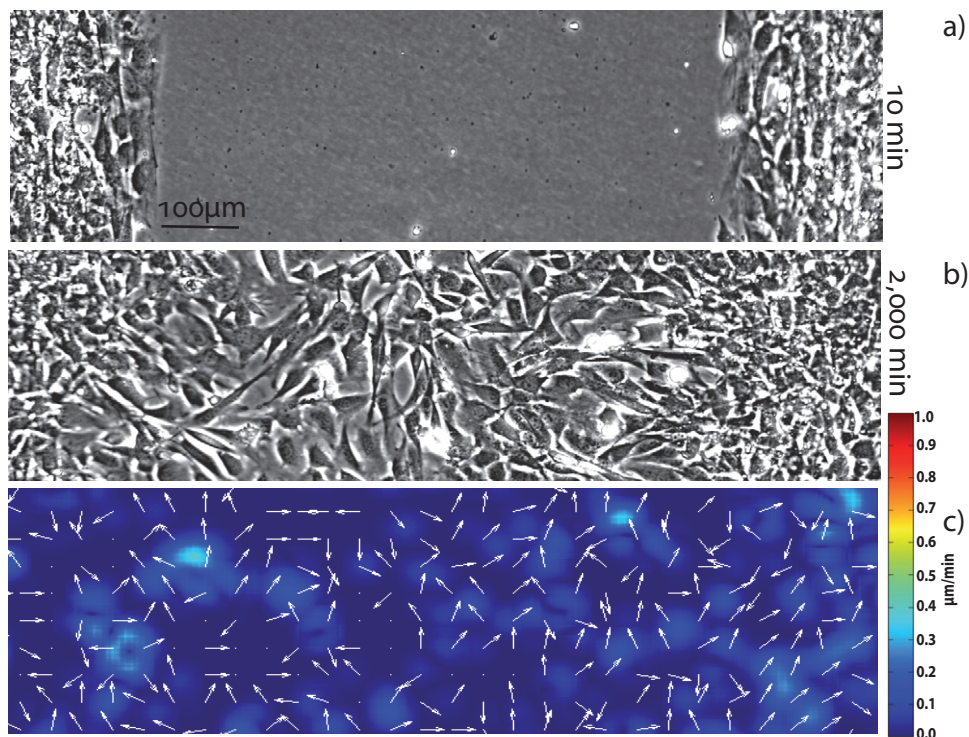
Figure 3. Phase contrast images of NIH-3t3 cells at various times. Panels (a) and (b) are the phase contrast images of the monolayer at times 10 and 2000 min, respectively. Panel (c) is the velocity distribution of the monolayer and the direction of displacement (white arrows) corresponding to (b). The velocity of the monolayer was generally lower compared to the MCF-10 monolayer. There was mixing of the monolayers when both oppositely migrating monolayers met.

a constant cell front on longer times because of the monolayer's ability to catch up with escaping single cells [12]. However, when both monolayers met, a transition from directed to random motion of the cells at the borderline of both sheets became evident (figure 2(c)). Cell migration was hampered and finally stopped. Therefore, the establishment of a defined cell boundary, when oppositely migrating cells met, was initiated by the jamming of cells within the monolayers.

To investigate the effect of the dynamics on the ability of the monolayer to form a constant cell front, we repeated the experiment by letting two sheets of NIH-3t3 fibroblast cells migrate into each other. As can be seen in figure 3, NIH-3t3 cells did not migrate as a monolayer with a constant cell front (see also supplementary movie 3, available from stacks.iop.org/NJP/14/115012/mmedia). Rather, single cells escaped from the monolayer and moved randomly in front of the sheet. In contrast to the epithelial cell monolayer, there was no global uni-directional motion of the fibroblasts within the monolayer in the direction of escaping single cells. Thus, the monolayer was not able to catch up with the escaping cells, and consequently, no boundary at the margin of the monolayer was developed.

Our investigations on MCF-10A and MCF-7 epithelial cells suggest that jamming of cells within a 2D sheet results in the establishment of boundaries during collective cell migration and prevents the mixing of the cells originating from different monolayers no matter the cell type.

The dynamics of the monolayer seems to play a dominant role in establishing a permanent cell front in 2D monolayers. When the cells are strongly interacting, such that single cells cannot escape, there is a permanent cell boundary preventing the mixing up of cells when two cell fronts meet (figure 1). In contrast, for weakly interacting epithelial cells, where single cells can escape the monolayer, the interplay between the ballistic motion of the monolayer and the random motion of the escaping cells enables the monolayer to catch up with the escaping cell, thereby retaining a constant cell front. Thus, the impact of a line tension in maintaining the permanent cell front is minimal. For non-interacting cells such as fibroblast, collective migration was theoretically shown to be an emergent property of single cell motion [26]. Although non-interacting single cells move as persistent random walkers, at very high densities, collisions between the cells can initiate collective motion [26, 27]. However, in a wound healing assay, the density reduces as single cells randomly move away from the monolayer and this prevents collective motion in non-interacting cells (figure 3(c)). Our study therefore shows that in two dimensions, when cells move collectively with a constant cell front, their jammed nature prevents two oppositely migrating monolayer from mixing up.

3.2. Glass-like features in the wound healing assay

The observed jammed behavior of cells exhibits features typical of a glass-like system; similar to collective cell migration that displays glass-like features when the density of the monolayer increases [23, 28]. However, the application of glass-like dynamics on cellular motion is complicated because of the soft and out-of-equilibrium nature of cells; e.g. the transition to a glass-like state when two cell monolayers meet could be slower than for hard spheres. Features typical of glassy systems include non-Arrhenius relaxation times and a slow and heterogeneous dynamics with increasing cell density. Additionally, heterogeneous dynamics, as described for glassy systems earlier [29–31], were already observed in our experiments at the interface of two monolayers as shown in figures 1(c) and 2(c). To investigate the glass-like nature in more detail, we studied the dynamics of the MCF-10A monolayer at a low (5×10^{-3} cells cm^{-2}) and a high (2×10^5 cells cm^{-2}) cell density (figure 4).

For both cell densities of MCF-10A cells, initially isotropic displacement fields were observed, that is, cells moved randomly on short times (figures 4(a) and (b)) with an average velocity below 0.4 μm min^{-1}. The random dynamics originated from local single cell rearrangements within the sheet. Besides the short time isotropic dynamics of the cells, the integrity of the monolayer was retained through cell–cell coupling. Thus, the cell monolayer moved into the direction of free space on long times (figures 4(c) and (d)).

On long times and for both cell densities, the displacement fields gradually changed from an isotropic to a directed pattern (figures 4(c) and (d)) with cells moving super-diffusively or ballistically. Furthermore, the spatial variation in magnitude of the velocity increased with time and was generally greater for the low cell density (figure 5(a)) in comparison to the high density (figure 5(b)). This increase in the width of the velocity distribution with time at a low cell density (figures 4(d) and 5(a)) correlates with an increase in cell surface area, which might initiate a larger cell density fluctuation. The decrease in cell density initiated by cell spreading also led to single cells dissociating from the monolayer on very long times (figure 4(c)). However, at higher cell density, cell dissociation was not observed. In contrast, we obtained a decreasing velocity gradient from the front of the sheet, where cells are more spread, to the back where cells are more crowded and less spread (figures 4(d) and 5(b)). For both cell densities,
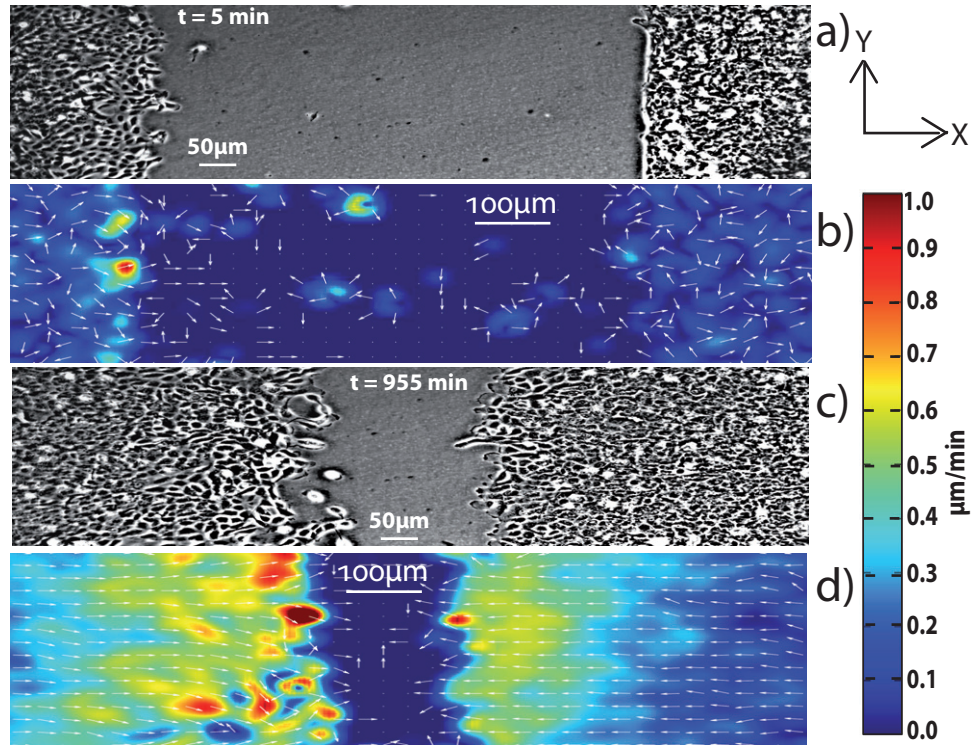
Figure 4. Dynamic heterogeneity at low (left) and high (right) cell densities. (a) Phase contrast image of cells seeded at a low and a high density at $t = 5$ min. (b) Random spatial distribution of cell velocity (color coded) and the displacement field of the monolayer (arrows) at $t = 5$ min. (c) Phase contrast image of cells seeded at a low and a high density 955 min after the measurement started. (d) Spatially heterogeneous velocity distribution of cells in the migrating sheet at $t = 955$ min. The displacement fields are uni-directional, thus suggesting ballistic motions.

there was a spatially heterogeneous dynamics, which is typical of a glass-like system and emanates from the cooperative motion of cells, i.e. faster cells move together, while slower cells stick together.

3.3. Intramonolayer dynamics

The comparison of epithelial and fibroblast cell motion showed that a stable cell boundary cannot be maintained if cells move randomly as individual cells. To determine the collectivity in migration of MCF-10A cells, we calculated the spatial velocity autocorrelation at various times. The spatial velocity autocorrelation was defined as

$$C(\delta x)_t = \frac{\langle v_y(x) \cdot v_y(x + \delta x) \rangle}{\langle v_y(x) \cdot v_y(x) \rangle}, \tag{3}$$

where $v = (r(t + \delta t) - r(t)) / (\delta t)$ and $r(t)$ defined in equation (2) is the position of a cell at some time (t) determined from equation (1). $\langle \cdots \rangle$ is the mean of the velocity in the y-direction.
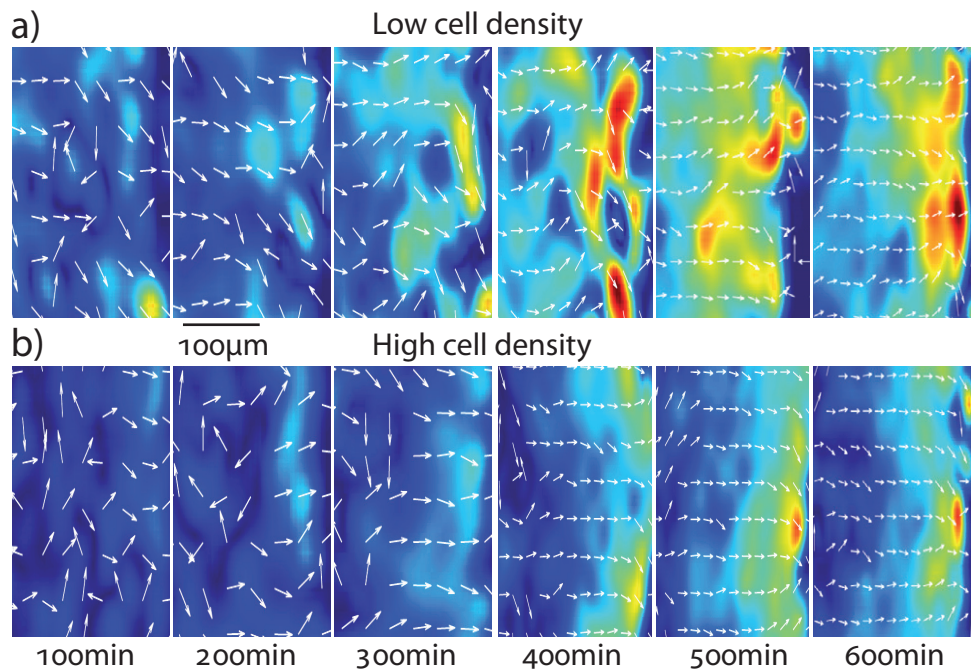
Figure 5. Temporal development of spatial velocity heterogeneity. (a) A cell sheet at a low density attains higher velocities more quickly and shows a more heterogeneous spatial velocity distribution. (b) The spatial velocity distribution of a larger density is less heterogeneous and the cells need a longer time to attain high velocities.

The velocity autocorrelation was best fitted by the Kohlrausch–William–Watts function of the form $C(x)_t = C_0 \exp\left(-\left(x/x_0(t)\right)^{\beta(t)}\right)$ (figures 6(a) and (b)). x_0 is the correlation length and β the compressing exponent. The mean of the compressing exponent β was 1.79 ± 0.14 for low cell density and 1.50 ± 0.24 at high cell density (figure 6(d)). The small values of β at short times at high cell density emanate from noise induced by cell media flows. The correlation length increased from a cell's diameter on short times to a maximum of about 10 cell diameters at long times (figure 6(c)). The increase in correlation length with time could result from the fact that at short times, the monolayer is stationary. As time increases, marginal cells start moving and this movement unjams the monolayer, since crowding suppresses the translation of cells. When the monolayer is unjammed, sub-marginal cells start moving; thus, spatial correlation increases with time, since the unjamming process is time dependent.

The increase of the correlation length with time agrees with studies on the collective motion of cells using Madin–Darby canine kidney (MDCK) cells with stronger intercellular coupling [10]. In this study, the correlation length also increased linearly with time for cells migrating on a poly-acrylamide gel, and the increase in correlation length with time was shown to correlate with increasing cell density. However, on a glass substrate, the correlation length decreased with increasing cell density (the cell density increases with time as a result of cell divisions). It should however be noted that, while the center of the monolayer was considered in the study using the MDCK cells, we performed a wound-healing-like assay on the glass substrate. By considering the center of the monolayer, the density of the system increases over time, which initiates swirls and dynamic arrest [23], causing changes in the spatial velocity
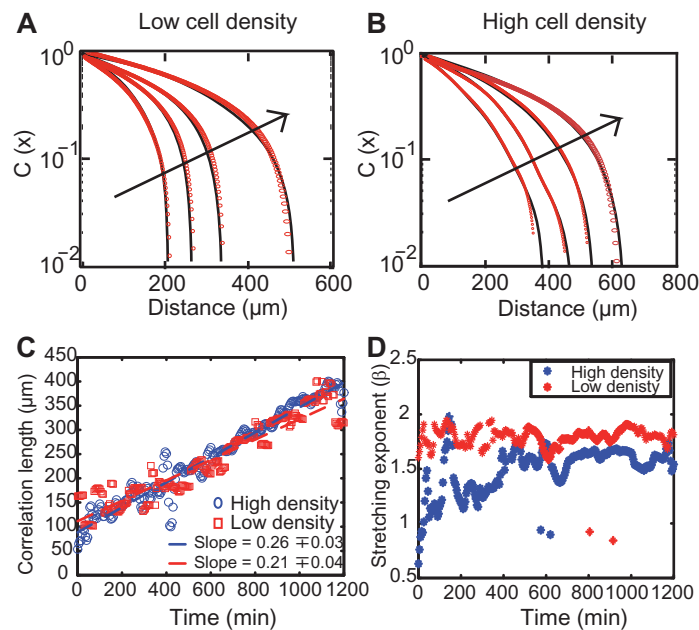
Figure 6. (a), (b) The spatial velocity autocorrelation function and fit (red) for increasing times as indicated by the arrow (200, 560, 750 and 1275 min) at a low (a) and a high (b) cell density. (c) The correlation length increases linearly with time for both cell densities. (d) The time evolution of the compressing exponent, which increased from 0.5 at short times to an average of 1.5 at long times for high cell density and remained fairly constant at 1.79 for small cell density.

correlation. In contrast, in a wound-healing-like assay, a density gradient is established as the monolayer migrates [12]. Using the MDCK cells in a wound healing assay, the correlation length was found to be about $200 \, \mu m$, after 5 h of migration [6]; this is of the same order of magnitude as compared to our study.

The compressed exponentials for the spatial correlation length, which we found for this actively spreading cell monolayer, are typical of passive nematic liquid crystals with correlated quenched disorder [32]. Such systems show long-range directional order and their temporal dynamics is similar to that of aging glassy colloids [33]. Moreover, compressed exponential relaxation times ($\beta = 1.5$) were observed in other soft matter systems such as colloidal gels [34, 35] and clays [36], and charged colloids with stronger inter-particle interactions showed $\beta > 1.5$ [37]. This compressed exponential behavior was heuristically modeled in terms of ultraslow, large-length-scale ballistic motions of elastic deformations in response to a local and spatially heterogeneous stress source [34, 38]. This is the same ballistic motion that we find in our cell monolayer, which might explain the compressed exponential correlation lengths in our system.

4. Discussion and conclusions

In this study, we have shown for the first time that the dynamical properties of cells play a crucial role in maintaining the establishment of a permanent cell front during collective migration and

the prevention of cellular mixing from different monolayers. For cells with strong intercellular interactions, it is obvious that single cells cannot escape the monolayer and a boundary is formed, suppressing the mixing up of cells when counter-migrating monolayers meet. However, even for weakly interacting cells, dynamic effects contribute in retaining a constant cell front. The ballistic motion of weakly coupled cells within a monolayer allows the moving sheet to catch up with single escaping cells, since these cells lose their super-diffusive behavior and migrate randomly [12]. Thus, for weakly interacting cells such as MCF-10A epithelial cells, the boundary is retained by the combination of the intercellular interactions and dynamic effects.

Moreover, we have shown that the formation of a permanent migratory front also acts as a dynamically induced barrier of jammed cells. According to the differential adhesion hypothesis, cohesion differences between two cell types result in the formation of 3D spheroids [39, 40] and demixing, while cells with lower cohesion forces and surface tension surround the other cell type [15, 41, 42]. Our investigations show for the first time that for a 2D cell sheet, differential adhesion and line tension differences originating from the fluid-like behavior of cells as described earlier [14, 43–45] are not a prerequisite for a stabilization of cell fronts. Since cells of the same type did not mix in our experiments, even an extended differential adhesion hypothesis [16] where the line tension is modulated by contractility cannot explain our findings. Here, dynamic effects in concert with intercellular interactions lead to jamming, which creates a line tension preventing single cells from escaping the cell monolayer and can act as a cell mixing suppressor by stabilizing the monolayer boundary. Since surface tension differences are expected not only to contribute to cellular behavior in three dimensions, but also in a 2D monolayer and especially at the interface of two monolayers, we show that other active physical properties can contribute to boundary stabilization besides passive line tension and adhesion forces.

In two dimensions, it has to be taken into account that the additional cell–substrate interaction determines if the cells round up into a 3D tissue or spread on the substrate and migrate [46]. If the intercellular interactions are too weak compared to cell adhesion to the substrate, no intact monolayer can be formed, and cells migrate randomly and escape from their neighbors as observed for NIH-3t3 fibroblast cells [18, 20]. Since the diffusive dynamics of these cells prevents jamming, no permanent cell front is formed and cells mix upon meeting another sheet of randomly moving cells.

The behavior of epithelial cells at the front when two monolayers meet can be described not only in terms of a transition from super-diffusive, directed motion to random motion, but also by considering glass-like features. Glass-like behavior such as the observed jammed nature of strongly interacting cells is characterized by heterogeneous dynamics, namely cells with higher velocity moving together at the cell front [10, 23] and starting to jam as soon as the directed motion is hampered. Moreover, we observed that the correlation lengths increased with time and are fitted well by compressed exponential Kohlrausch–William–Watts functions, characteristic of aging glassy systems. The increased correlation length with time suggests that the dynamics is highly coordinated and spans several cell lengths.

Interestingly, our study suggests that glass-like dynamics and jamming surprisingly occur within the actively moving and deformable cell monolayer system. Generally, glassy behavior is described by cooling or crowding passive systems, while the underlying dynamics and nature of glassy systems are not well understood. We can only assume that cell divisions and migration acting as external heterogeneous stress sources simultaneously jam and shear [8, 23, 47] the monolayer, respectively. Cell migration-induced shear stresses are heterogeneously

transmitted [8, 9] through cell–cell couplings to neighboring cells, which are consequently deformed and aligned [6, 48] over a long distance. Cell deformation pre-strains the cells, which thereby results in a slight stiffening of the entire monolayer. The stiffening enables a long-range transmission of shear forces through intercellular couplings. Long-ranged force transmissions culminate in collective cell motion, which consequently jams the monolayer.

The observed jamming and glass-like dynamics are expected not only to play a crucial role in embryologic development, but also in the progression of a tumor since it can be considered a developing tissue. Höckel employed the term *ontogenetic anatomy* which maps the human body from its embryological origin (anlage) and characterizes the compartments representing morphogenetic units in the adult [49, 50]. Here the compartment boundaries are primary proliferation and migration suppressors. Höckel could clearly show that women with non-metastatic carcinomas of the uterine cervix originating in the Müllerian compartment have a reduced mortality from 20 to 4% when the total compartment is resected even without subsequent radiation or chemotherapy [49, 51, 52]. Following his compartment theory, cells of the primary tumor have the ability to spread and migrate freely within their initial ontogenetic compartment where the tumor originated because tumor cells and normal cells behave similarly. Only major changes of the tumor cells such as epithelial–mesenchymal transitions are a prerequisite of tumor progression beyond compartment borders and subsequently metastasis. Since within such a compartment, normal cells and tumor cells do not necessarily demix as proposed by the differential adhesion hypothesis, the question of what keeps the tumor cells inside their host compartments might similarly be answered as observed in our experiments: intercellular interactions and dynamic effects stabilize compartment boundaries, while jamming can further act as a proliferation suppressor [18–20] due to a lack of space and increased homeostatic pressure [53]. To this end, future studies will focus on the dynamics of cells not only in 2D, but in 3D systems. Droplet cultures can be employed to investigate the origin of mixing and demixing in correlation with surface tension differences to understand why cancer cells can gain the ability to leave the host tumor and metastasize. Nevertheless, since Wicki *et al* showed that upregulation of podoplanin—a small mucin-like protein—of cells at the tumor front promotes invasion in the absence of epithelial–mesenchymal transition by the formation of filopodia [54], it becomes evident that tumor progression might be mainly determined by the underlying dynamics of single cells within the entire system, even without major changes in cell–cell interaction.

Acknowledgments

References

[1] Friedl P 2004 Prespecification and plasticity: shifting mechanisms of cell migration *Curr. Opin. Cell Biol.* **16** 14–23
[2] Friedl P and Gilmour D 2009 Collective cell migration in morphogenesis, regeneration and cancer *Nature Rev. Mol. Cell Biol.* **10** 445–57

[3] Omelchenko T, Vasiliev J M, Gelfand I, Feder H H and Bonder E M 2003 Rho-dependent formation of epithelial 'leader' cells during wound healing *Proc. Natl Acad. Sci. USA* **100** 10788–93

[4] Poujade M, Grasland-Mongrain E, Hertzog A, Jouanneau J, Chavrier P, Ladoux B, Buguin A and Silberzan P 2007 Collective migration of an epithelial monolayer in response to a model wound *Proc. Natl Acad. Sci USA* **104** 15988–93

[5] Vitorino P and Meyer T 2008 Modular control of endothelial sheet migration *Genes Dev.* **22** 3268–81

[6] Petitjean L, Reffay M, Grasland-Mongrain E, Poujade M, Ladoux B, Buguin A and Silberzan P 2010 Velocity fields in a collectively migrating epithelium *Biophys. J.* **98** 1790–800

[7] Vitorino P, Hammer M, Kim J and Meyer T 2011 A steering model of endothelial sheet migration recapitulates monolayer integrity and directed collective migration *Mol. Cell. Biol.* **31** 342–50

[8] Tambe D T *et al* 2011 Collective cell guidance by cooperative intercellular forces *Nature Mater.* **10** 469–75

[9] Trepat X, Wasserman Angelini T E, Millet E, Weitz D A, Butler J P and Fredberg J J 2009 Physical forces during collective cell migration *Nature Phys.* **5** 426–30

[10] Angelini T E, Hannezo E, Trepat X, Fredberg J J and Weitz D A 2010 Cell migration driven by cooperative substrate deformation patterns *Phys. Rev. Lett.* **104** 168104

[11] Fritsch A, Hockel M, Kiessling T, Nnetu K D, Wetzel F, Zink M and Käs J A 2010 Are biomechanical changes necessary for tumour progression? *Nature Phys.* **6** 730–2

[12] Nnetu K D, Knorr M, Strehle D, Zink M and Käs J A 2012 Directed persistent motion maintains sheet integrity during multi-cellular spreading and migration *Soft Matter* **8** 6913–21

[13] Steinberg M S 1963 Reconstruction of tissue by dissociated cells *Science* **141** 401–8

[14] Foty R A, Forgacs G, Pfleger C M and Steinberg M S 1994 Liquid properties of embryonic tissues: measurement of interfacial tensions *Phys. Rev. Lett.* **72** 2298–301

[15] Foty R A and Steinberg M S 2005 The differential adhesion hypothesis: a direct evaluation *Dev. Biol.* **278** 255–63

[16] Manning M L, Foty R A, Steinberg M S and Schoetz E M 2010 Coaction of intercellular adhesion and cortical tension specifies tissue surface tension *Proc. Natl Acad. Sci. USA* **107** 12517–22

[17] Ramis-Conde I, Drasdo D, Anderson A R A and Chaplain M J A 2008 Modeling the influence of the e-cadherin-beta-catenin pathway in cancer cell invasion: a multiscale approach *Biophys. J.* **95** 155–65

[18] Martz E 1973 Contact inhibtion of speed in 3t3 and its independence from postconfluence inhibition of cell divisions *J. Cell Physiol.* **81** 39–48

[19] Martz E, Phillips H M and Steinberg M S 1974 Contact inhibition of overlapping and differential cell adhesion: a sufficient model for the control of certain cell culture morphologies *J. Cell Sci.* **16** 401–19

[20] Martz E and Steinberg M S 1974 Movement in a confluent 3t3 monolayer and the causes of contact inhibition of overlapping *J. Cell Sci.* **15** 201–16

[21] Sommers C L, Byers S W, Thompson E W, Torri J A and Gelmann E P 1999 Differentiation state and invasiveness of human breast cancer cell lines *Breast Cancer Res. Treat.* **31** 325–35

[22] Mierke C T, Frey B, Fellner M, Herrmann M and Fabry B 2010 Integrin $\alpha 5 \beta 1$ facilitates cancer cell invasion through enhanced contractile forces *J. Cell Sci.* **124** 369–83

[23] Angelini T E, Hannezo E, Trepat X, Marquez M, Fredberg J J and Weitz D A 2011 Glass-like dynamics of collective cell migration *Proc. Natl Acad. Sci. USA* **108** 4714–9

[24] Betz T, Koch D, Lim D and Käs J A 2009 Stochastic actin polymerization and steady retrograde flow determine growth cone advancement *Biophys. J.* **96** 5130–8

[25] Knorr M, Koch D, Fuhs T, Behn U and Käs J A 2011 Stochastic actin dynamics in lamellipodia reveal parameter space for cell type classification *Soft Matter* **7** 3192–203

[26] Bindschadler M and McGrath J L 2007 Sheet migration by wounded monolayers as an emergent property of single-cell dynamics *J. Cell Sci.* **120** 876–84

[27] Szabó B, Szöllösi G J, Gönci B, Jurányi Zs, Selmeczi D and Vicsek T 2006 Phase transition in the collective migration of tissue cells: experiment and model *Phys. Rev.* E **74** 061908

[28] Henkes S, Fily Y and Marchetti M C 2011 Active jamming: self-propelled soft particles at high density *Phys. Rev.* E **98** 040301

[29] Silbert L E 2005 Temporally heterogeneous dynamics in granular flows *Phys. Rev. Lett.* **94** 098002

[30] Dauchot O, Marty G and Biroli G 2005 Dynamical heterogeneity close to the jamming transition in a sheared granular material *Phys. Rev. Lett.* **95** 265701

[31] Garrahan J P 2011 Dynamic heterogeneity comes to life *Proc. Natl Acad. Sci. USA* **108** 4701–2

[32] Nespoulous M, Blanc C and Maurizio N 2010 Orientational quenched disorder of a nematic liquid crystal *Phys. Rev. Lett.* **104** 097801

[33] Marinelli M, Mercuri F, Paoloni S and Zammit U 2005 Dynamics of nematic liquid crystal with quenched disorder in the random dilution and random field regimes *Phys. Rev. Lett.* **95** 237801

[34] Cipelletti L, Manley S, Ball R C and Weitz D A 2000 Universal aging features in the restructuring of fractal colloidal gels *Phys. Rev. Lett.* **84** 2275–8

[35] Ramos L and Cipelletti L 2001 Ultraslow dynamics and stress relaxation in the aging of a soft glassy system *Phys. Rev. Lett.* **87** 245503

[36] Bandyopadhyay R, Liang D, Yardimci H, Sessoms D A, Borthwick M A, Mochrie S G J, Harden J L and Leheny R L 2004 Evolution of particle-scale dynamics in an aging clay suspension *Phys. Rev. Lett.* **93** 228302

[37] Fischer B, Wagne J, Gutt C, Westermeier F and Gübel G 2010 Structure and dynamics of glassy charged colloids studied with coherent small angle x-ray scattering *J. Phys.: Conf. Ser.* **247** 012026

[38] Cipelletti L, Ramos R, Manley S, Pitard E, Weitz E E, Pashkovsk D A and Johansson M 2003 Universal non-diffusive slow dynamics in aging soft matter *Faraday Discuss.* **123** 237–51

[39] Douezan S and Brochard-Wyart F 2012 Dewetting of cellular monolayers *Eur. Phys. J. E* **35** 1–6

[40] Douezan S and Brochard-Wyart F 2012 Active diffusion-limited aggregation of cells *Soft Matter* **8** 784–8

[41] Foty R A and Steinberg M S 2004 Cadherin-mediated cell–cell adhesion and tissue segregation in relation to malignancy *Int. J. Dev. Biol.* **48** 397–409

[42] Duguay D, Foty R A and Steinberg M S 2003 Cadherin-mediated cell adhesion and tissue segregation: qualitative and quantitative determinants *Dev. Biol.* **253** 309–23

[43] Dobereiner H-G, Dubin-Thaler B, Giannone G, Xenias H S and Sheetz M P 2004 Dynamic phase transitions in cell spreading *Phys. Rev. Lett.* **93** 108105

[44] Dubin-Thaler B J, Giannone G, Dobereiner H G and Sheetz M P 2004 Nanometer analysis of cell spreading on matrix-coated surfaces reveals two distinct cell states and STEPs *Biophys. J.* **86** 1794–806

[45] Fardin M A, Rossier O M, Rangamani P, Avigan P D, Gauthier N C, Vonnegut W, Mathur A, Hone J, Iyengar R and Sheetz M P 2010 Cell spreading as a hydrodynamic process *Soft Matter* **6** 4788–99

[46] Ryan P L, Foty R A, Kohn J and Steinberg M S 2001 Tissue spreading on implantable substrates is a competitive outcome of cell–cell versus cell–substratum adhesivity *Proc. Natl Acad. Sci. USA* **98** 4323–7

[47] Ranft J, Basan M, Elgeti J, Joanny J F, Prost J and Jülicher F 2010 Fluidization of tissues by cell division and apoptosis *Proc. Natl Acad. Sci. USA* **107** 20863–8

[48] Reffay M, Petitjean L, Coscoy S, Grasland-Mongrain E, Amblard F, Buguin A and Silberzan P 2011 Orientation and polarity in collectively migrating cell structures: statics and dynamics *Biophys. J.* **100** 2566–75

[49] Höckel M, Schmidt K, Bornmann K, Horn L-C and Dornhöfer N 2010 Vulvar field resection: novel approach to the surgical treatment of vulvar cancer based on ontogenetic anatomy *Gynecol. Oncol.* **119** 106–13

[50] Höckel M 2012 Cancer permeates locally within ontogenetic compartments: clinical evidence and implications for cancer surgery *Future Oncol.* **8** 29–36

[51] Höckel M, Horn L C and Fritsch H 2005 Association between the mesenchymal compartment of uterovaginal organogenesis and local tumour spread in stage ib–iib cervical carcinoma: a prospective study *Lancet Oncol.* **6** 751–6

[52] Höckel M, Horn L-C, Manthey N, Braumann U-D, Wolf U, Teichmann G, Frauenschlager K, Dornöfer N and Einenkel J 2009 Resection of the embryologically defined uterovaginal (Müllerian) compartment and pelvic control in patients with cervical cancer: a prospective analysis *Lancet Oncol.* **10** 683–92

[53] Basan M, Risler T, Joanny J-F, Sastre-Garau X and Prost J 2009 Homeostatic competition drives tumor growth and metastasis nucleation *HFSP J.* **3** 265–72

[54] Wicki A, Lehembre F, Wick N, Hantusch B, Kerjaschki D and Christofori G 2006 Tumor invasion in the absence of epithelial–mesenchymal transition: podoplanin-mediated remodeling of the actin cytoskeleton *Cancer Cell* **9** 261–72